Organic Process Research & Development

ARTICLE

pubs.acs.org/OPRD

In-Process Monitoring and Control of Supersaturation in Seeded Batch Cooling Crystallisation of L-Glutamic Acid: From Laboratory to Industrial Pilot Plant

Shahid Khan, Cai Y. Ma, Tariq Mahmud,* Radoslav Y. Penchev,† and Kevin J. Roberts

Institutes of Particle Science and Engineering and of Process Research and Development, School of Process, Environmental and Materials Engineering, The University of Leeds, Leeds LS2 9JT, U.K.

Julian Morris and Leyla Özkan‡

Centre for Process Analytics and Control Technology (CPACT), School of Chemical Engineering and Advanced Materials, The University of Newcastle, Newcastle NE1 7RU, U.K.

Graeme White

School of Engineering and Physical Sciences, Heriot-Watt University, Edinburgh EH14 4AS, U.K.

Bruce Grieve§ and Alan Hall

Syngenta, Huddersfield Manufacturing Centre, PO Box A38, Leeds Road, Huddersfield HD2 1FF, U.K.

Paul Buser, Neil Gibson, and Patrik Keller

Syngenta Crop Protection, Münchwillen AG, Breitenloh 5, CH-4333 Münchwillen, Switzerland

Paul Shuttleworth

HEL Limited, 50 Moxon Street, Bernet, Hertfordshire EN5 5TS, U.K.

Christopher J. Price

Particle Sciences Group, GlaxoSmithKline, Stevenage SG1 2NY, U.K.

ABSTRACT: A measurement-based closed-loop control system using in-process ATR-FTIR spectroscopy coupled with a multivariate chemometric PLS calibration model is developed, validated, and applied to the monitoring and control of supersaturation in a 250- L industrial pilot-plant crystalliser. Supersaturation control experiments are carried out on seeded batch cooling crystallisation of β-L-glutamic acid from aqueous solutions using two methods of seeding involving addition of seeds to the solution and generation of seeds within the solution. The generic applicability of the approach is demonstrated through this challenging system reflecting this molecule's weak chromophore for infrared and relatively low solubility compared with previous solute−solvent systems. Based on the laboratory experiments, the system was fully tested and optimised prior to a series of trials carried out in an industrial pilot plant at Syngenta, Münchwillen, Switzerland. Good control of the supersaturation is achieved at three levels, 1.1, 1.2, and 1.3, within a prescribed range of ±0.025. The average product crystal size is found to decrease with increasing supersaturation. Comparison between product crystals produced at the 20- and 250-L scales indicates that secondary nucleation is more prevalent at the smaller-scale size. For the same level of supersaturation, the rate of depletion of solute is faster at the 20-L scale size than at 250-L scale, and hence a higher cooling rate is required to maintain the desired supersaturation. However, for a given crystalliser scale size, as expected, the mean cooling rate required to maintain a constant supersaturation is found to increase with increasing supersaturation level.

1. INTRODUCTION

Crystallisation is a major unit operation used for the formulation and isolation of wide-ranging solid products, for example, in the agrochemicals, fine chemicals and active pharmaceutical ingredients manufacturing industries. Most of these solid materials are manufactured by batch cooling crystallisation processes with the aim to meet desired product specifications, e.g., narrow crystal

Received: August 13, 2010
Published: March 14, 2011

size distribution (CSD), high crystal purity, optimum crystal morphology and high yield, which can also facilitate efficient downstream processing such as filtration, drying and milling. These specifications need to be met consistently in order to avoid batch-to-batch variations. The development of a reliable and reproducible industrial crystallisation process in the laboratory and its scaling-up to an industrial scale poses serious fundamental as well as practical challenges for the production of many speciality materials, particularly, organic solids. In a crystallisation process, supersaturation provides the required driving force for nucleation and crystal growth, both of which accelerate as the level of supersaturation increases. It is therefore desirable to minimise the extent of nucleation process and maximise the crystal growth so that most of the material dissolved in the solution can accumulate on the surfaces of a small number of crystals in order to obtain the required CSD. This can be achieved by controlling the level of supersaturation during the crystallisation process. Nucleation is dominant at high supersaturation levels whereas crystal growth can occur and proceed at considerably lower levels of supersaturation.[1] Based on these considerations, the most favorable crystal properties may be achieved if the supersaturation is kept constant at a relatively low level throughout the crystallisation process. Controlling batch cooling crystallisation processes via this approach requires a combination of accurate online measurements of analyte concentration and therewith supersaturation together with the use of an appropriate control algorithm to sustain the required levels of supersaturation for the following nucleation and crystal growth processes.

Various methods have been developed and implemented in industrial processes to control supersaturation,[2,3] which includes seeding, programmed cooling, programmed feeding rates of reactants in precipitation processes, and solvent evaporation. In order to maintain a required level of supersaturation via the use of controlled cooling modes, which is the focus of this study, it is necessary to apply a suitable temperature profile, which requires development of an operating strategy that should depend on the system parameters and process conditions.[4] In previous studies, different cooling profiles have been employed in batch crystallisation processes at laboratory-scale sizes, which include natural,[5−9] linear[5−13] and controlled[5−14] cooling. In natural cooling, the solution is cooled using a coolant with a constant inlet temperature resulting in an exponential decay in the solution temperature with time. Consequently, the solution is usually supersaturated at a considerably faster rate than it is possible to desupersaturate by the nucleation and subsequent growth of the existing crystals.[6] This can cause the supersaturation to build up very rapidly in the early stages and then drop when nucleation occurs after exceeding the metastable limit leading to a largely uncontrolled crystallisation process resulting in a wider CSD than desired with a significant number of small, irregularly shaped crystals in the product.[4] Linear cooling involves cooling of the solution at a constant rate throughout the whole crystallisation process. If the cooling rate is too fast, the supersaturation may significantly exceed the metastable limit, leading to worsening quality of the product as a consequence of uncontrolled nucleation. On the other hand, too slow cooling rates can result in uneconomically long batch times. Judicious application of constant cooling rates may reduce the generation of high level of initial supersaturation associated with natural cooling and hence the occurrence of spontaneous nucleation which leads to an increase in the average crystal size through promoting the crystal growth.[6] However, this may require a number of trial and error experiments to find an optimum cooling rate and, in any case, due to the heterogeneous nature of nucleation processes such a methodology would be very hard to scale up from laboratory to practical manufacture-scale sizes.

Efforts have been made by many researchers to find optimal cooling profiles that should be followed in order to carry out crystallisation processes in a controlled manner. The objective of using a programmed cooling profile is to ensure that the supersaturation generation rate always matches the available crystal surface area on to which the solute molecules in the solution are to be transferred.[15] This means that at the beginning of the crystallisation process, when the surface area of the existing crystals is small, the rate of generation of supersaturation has to be slow and therefore the applied cooling rates need to be low. As the crystallisation process progresses, the surface area of the crystals increases and the cooling rate should also increase. Mullin and Nyvlt[5] first proposed programmed cooling of batch crystallisation processes, later refined by Jones and Mullin,[6,14] who derived a theoretical equation, based on population balance modelling coupled with material and energy balances, from which an optimum cooling profile could be calculated. The programmed cooling profiles were used[5,6] in seeded crystallisation experiments with aqueous solutions of potassium sulphate and ammonium sulphate in laboratory-scale crystallisers. In both cases, the average crystal size increased compared with constant and natural cooling but a significant amount of fine crystals was also present in the products, revealing that the applied cooling profiles were not maintaining constant supersaturation probably due to poor control of secondary nucleation.

In order to control the crystal size and its distribution in batch cooling crystallisation processes, different measurement-based feedback (i.e., closed-loop) control strategies with various online supersaturation monitoring techniques have been developed and implemented in crystallisers of laboratory-scale sizes by a number of research groups (see for details[3]), which includes, amongst other techniques, the use of attenuated total reflection (ATR) Fourier transform infrared (FTIR) spectroscopy for real-time measurement and control of solute concentration, for example, by Grön et al.,[3] Liotta and Sabesan,[13] Feng and Berglund[16] and Fujiwara et al.[17] However, implementation of in-process monitoring and feedback control of supersaturation for industrial-scale crystallisation processes has yet to be realised.

Feng and Berglund[16] used a feedback control system together with ATR-FTIR using a peak-ratio calibration model to control the solution cooling rate in a 1-L jacketed crystalliser in order to maintain a low supersaturation level close to that of the solubility during cooling crystallisation of succinic acid. Fujiwara et al.[17] have implemented a control strategy together with online measurement of solution concentration using ATR-FTIR for the seeded crystallisation of paracetamol in a 500-mL jacketed crystalliser based on controlling the jacket water flow using a Proportional Integral (PI) control system in order to follow a prescribed absolute supersaturation (defined as $\Delta C = C - C^*$, where C is the solute concentration and C^* is the equilibrium concentration at the corresponding temperature) profile close to the metastable limit. The final product crystal size increased by minimising undesired nucleation. Grön et al.[3] have developed a closed-loop control strategy using ATR-FTIR for controlling the CSD associated with the crystallisation of monosodium glutamate (MSG) from aqueous solution at the 500-mL scale-size by maintaining the supersaturation ratio (defined as $S = C/C^*$) within a narrow range of a minimum and a maximum value. This was facilitated by manipulating the solution cooling rate in order

to control the balance between the nucleation and growth processes. This strategy has been used to control the supersaturation at different levels (S = 1.20 − 1.44), yielding a superior quality crystalline product with a narrow CSD, uniform crystal shape and a mean crystal size directly related to the supersaturation. The feedback control system developed by Liotta and Sabesan[13] and applied to crystallisation of a pharmaceutical compound in a 1-L vessel utilised a cascade of two control loops (primary and secondary) using a PI algorithm with ATR-FTIR being used to measure online solution concentration and absolute supersaturation. At each time interval and crystalliser temperature, the supersaturation was compared with the set-point with the solution cooling rate set-point being manipulated through the action of the primary control loop with cooling rate being translated into a new crystalliser temperature set-point. The secondary control loop then ensured that the updated temperature set-point specified by the primary loop was achieved by manipulating the heater/chiller. In this way, the supersaturation was able to be maintained at a constant set-point by continuously adjusting the crystalliser temperature. Compared with uncontrolled experiments the crystals obtained were significantly larger with low supersaturation levels resulting in growth being more pronounced leading to larger and more uniform crystals.

The study reported in this paper focuses on the further development and scale-up of the closed-loop supersaturation control approach developed earlier,[3] this time using ATR-FTIR coupled with a multivariate chemometric calibration model for controlling the batch cooling crystallisation of L-glutamic acid (LGA). This work has been carried out as part of a large collaborative research project with industry (*Chemicals Behaving Badly*, www.leeds.ac.uk/chemeng/CBB/cbb2.html) addressing the need for developing effective methods for online measurement and control of industrial crystallisation processes. In particular, the overall approach is scaled up for implementation initially at the 20-L laboratory-scale and then at the 250-L scale crystalliser. Crystallisation of this specific compound from aqueous solutions was selected as a model system as it provides significant challenge for the application of in-process ATR-FTIR spectroscopy for process control due to its very weak spectral features in the mid-IR frequency range, low aqueous solubility and complex speciation chemistry. This demanded the use of a more advanced multivariate chemometric partial least-squares (PLS) FTIR calibration model compared with that used in the previous study.[3] The model was developed and validated for the predictions of solution concentration from measured IR spectra and applied for the online monitoring of supersaturation variation during seeded batch cooling crystallisation of LGA at constant cooling rates in 500-mL and 20-L scale sizes.[18] Building on this work, the system was initially applied for controlling the supersaturation at constant levels in the 20-L crystalliser with the control algorithm parameters being optimised to provide a basis for further scale-up. The control system with associated process analytic probes was implemented in a 250-L scale pilot-plant crystalliser at Syngenta, Münchwillen, Switzerland to demonstrate its performance at an industrial scale through a series of trials carried out on the seeded batch cooling crystallisation of β-LGA at different levels of supersaturation.

2. MATERIALS AND METHODS

2.1. Materials. LGA (chemical formula: $C_5H_9NO_4$, molecular weight: 147.13 g/mol) is a α-amino acid with three functional groups for protonation/deprotonation, that is, two carboxylic acid groups and one basic amine group. In aqueous solutions, the molecule dissociates to yield four species; speciation chemistry is described in reference.[18] LGA has two well-defined polymorphic forms involving different molecular conformations and yielding different crystal morphologies: the metastable, more soluble and prismatic α-form and the stable, less soluble and needle-like β-form, as shown in Figure 1, a and b, respectively. This study is concerned with the latter form, which was supplied by VWR International (BDH) as powder (see Figure 1c) with stated purity of 99% and crystal size of $D_{0.5}$ = 132 μm and $D_{4,3}$ = 196 μm. Solutions were prepared using distilled and normal process water for the laboratory and pilot-plant experiments, respectively.

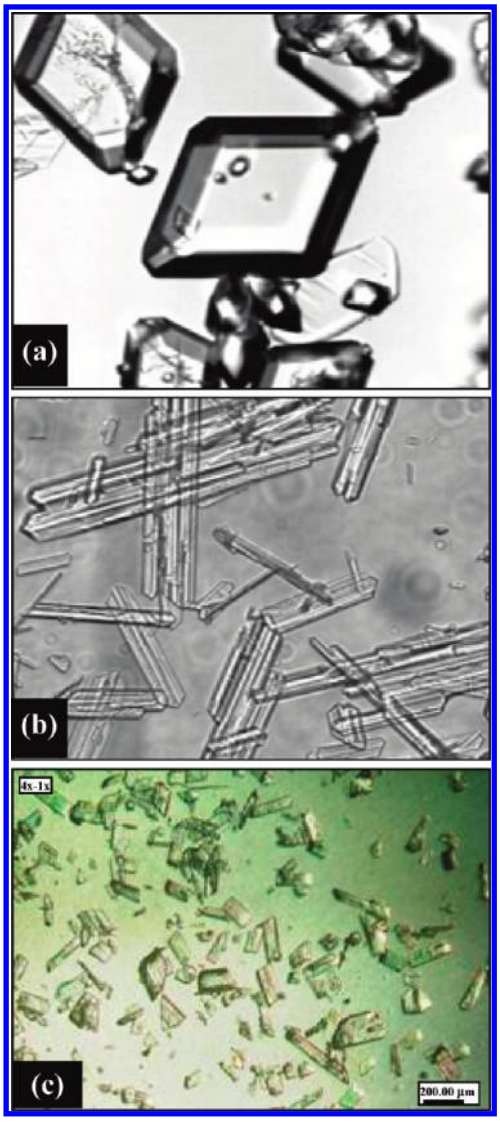

Figure 1. Microscopic images of (a) α-form and (b) β-form of LGA together with (c) β-LGA ($D_{0.5}$ = 132 μm and $D_{4,3}$ = 196 μm) as supplied by VWR International (BDH).

2.2. Experimental Setup. Laboratory experiments were carried out in Leeds using the HEL (Hazard Evaluation Laboratory Ltd.) AUTOLAB reactor system which consisted of a 20-L jacketed unbaffled stirred tank glass crystalliser with the temperature maintained and controlled using Huber Unistat 141

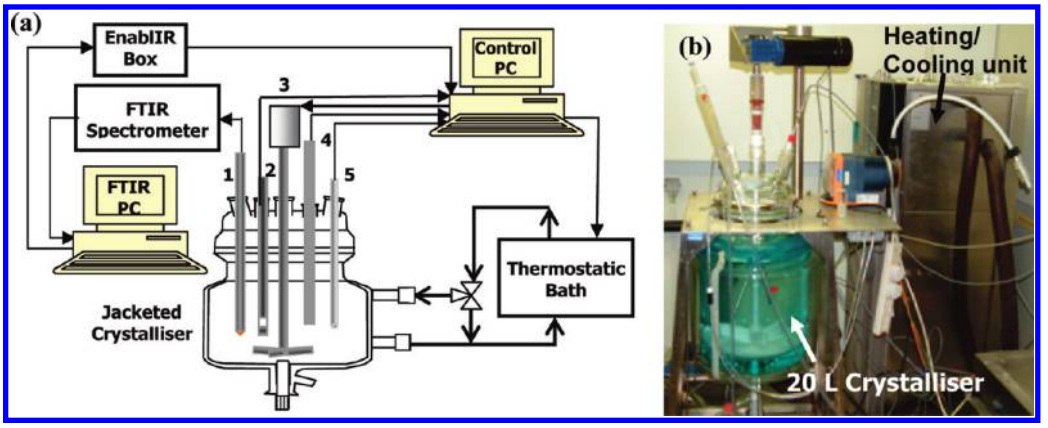

Figure 2. (a) Schematic of the 20-L crystalliser with associated instrumentations (1 - ATR probe, 2 - turbidity probe, 3 - stirrer motor, 4 - temperature probe, 5 - pH probe) and (b) photograph of the crystalliser and the heating/cooling unit.

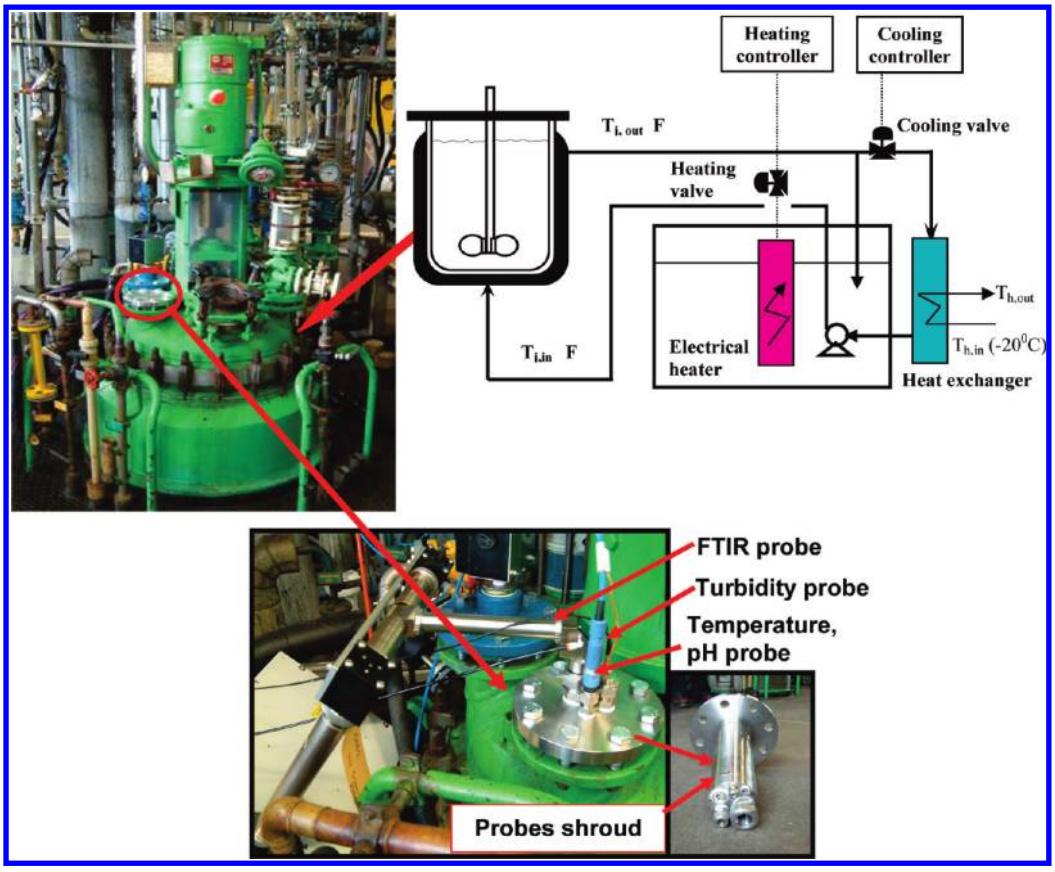

Figure 3. Schematic and photograph of the 250-L pilot-plant experimental facilities at Syngenta, Münchwilen, Switzerland.

heater/chiller thermostatic bath, a data interface board (A/D), and a PC running with HEL WinISO (version 2.3.29.2) process control software. The LGA solution was stirred using a PTFE retreat curve impeller operated at 100 rpm (corresponding to a Reynolds number, $Re = 6.1 \times 10^4$). An ATR-FTIR spectrometer, a platinum resistance thermometer (PT100), an in-house-built turbidimetric fibre-optic probe and a glass pH electrode were used to measure analyte concentration and temperature, turbidity (to detect the onset of crystallisation) and pH of the solution, with their output signals being logged by the control PC. The 20-L laboratory-scale experimental facility is shown schematically and by pictorial representation in Figure 2.

The industrial pilot-plant crystalliser at Syngenta, Münchwillen, Switzerland is shown in Figure 3. This is a standard glass-lined pressure vessel system fitted with a retreat curve impeller and a single beavertail baffle. The capacity of the crystalliser is 250 L with recommended maximum liquid volume of 225 L. The impeller speed was set to 100 rpm ($Re = 3.3 \times 10^5$). The same impeller speed in the 20- and 250-L vessels was used because the measured mixing times in both scale sizes were similar (~10 s). A Belatec heater/chiller unit was used for heating and cooling of the crystalliser contents. The process analytic probes for ATR-FTIR, pH, temperature, and turbidity were assembled into a specially designed shroud and flanged assembly, which was inserted into

dx.doi.org/10.1021/op100223a |*Org. Process Res. Dev.* 2011, 15, 540–555

the vessel through one of the reactor's top ports (see the inset in Figure 3). Reflux condensers were used for both the crystallisers to prevent loss of solvent due to evaporation.

2.3. ATR-FTIR Spectrometer and Calibration Model. For in situ measurements of solution concentration in both the 20- and 250-L scale sizes, mid-IR spectra were taken using an ABB Bomem WorkIR FTIR spectrometer coupled to a Dipper-210 ATR immersion probe equipped with a ZnSe conical internal reflection element manufactured by Axiom Analytical Inc. The spectrometer was connected via an Ethernet link to a control PC, equipped with EnablIR software (Galactic Industries Corp.), which facilitated the collection of FTIR spectroscopic data continuously and applied a PLS calibration model previously developed[18] to the data. The predicted concentration values were exported as 4−20 mA signals via an interface (EnablIR Box), see Figure 2, to the HEL control PC with WinISO software installed for the 20-L laboratory crystalliser or to the supersaturation control PC equipped with MATLAB software for the pilot-plant crystalliser via the plant's Foxboro control system. The solute concentration was measured at a fixed location in the pilot-plant crystalliser. The vertical position of the ATR probe tip was dictated by the probe length, which was placed midway between the impeller shaft and the vessel wall at a location approximately 0.1 m below the liquid surface. The computational fluid dynamic simulations of mixing in this crystalliser revealed that an essentially homogeneous environment exists for the agitation speed of 100 rpm ($Re = 3.3 \times 10^5$) used in the experiment. This suggests that the measured concentration was fairly representative of the whole volume of the crystalliser.

The LGA concentrations were predicted from the measured absorbance spectra using a multivariate chemometric PLS calibration model. The spectral data for building the calibration model and for its subsequent validation were collected from LGA solutions using a HEL 500 mL jacketed glass crystalliser over the concentration range of 3.0−62.5 g/L (0.02− 0.42 M) and temperature range: 40−90 °C, for details see ref 18. The spectral range used in the PLS model was 2000−1000 cm^{-1}. A number of spectra were taken in each solution, with each spectrum consisting of 64 scans at a spectral resolution of 8 cm^{-1}. A total of 168 spectra were used to build the model, with 34 independent spectra being used for model validation. The PLS method together with mean centring and the baseline correction were applied to build the model using the PLSplus IQ software (PLSplusIQ™, Thermo Galactic, 1991−2002, www.thermogalactic.com). The coefficient of correlation, R^2, was 0.9434 and the errors of prediction were in the range 1−10%. The model validation revealed that the standard deviation of the differences between the actual and predicted concentrations and the percentage error were 1.82 and 4.8%, respectively.

2.4. Crystallisation Procedure. Prior to use, the crystallisers and the probes were washed thoroughly with distilled or process water in order to ensure that there were no particles or residues left in the vessel from previous experiments. Normal process water used for experiments was charged into the pilot-plant crystalliser directly using a Batchmeter to record the total volume. An analytical balance (Mettler-Toledo Ltd.) was used to weigh the LGA powder for laboratory experiments, while an ordinary balance was used for the pilot-plant trials. Solutions were prepared by dissolving appropriate amounts of β-LGA in distilled water for the 20-L crystalliser and normal process water for the pilot-plant crystalliser. A dip can (a beaker with long handle) was inserted into the pilot-plant crystalliser through a manhole to collect slurry samples for analysis at the end of each experiment. The spectrometer, its conduits, and ATR probe were constantly purged with dry air or nitrogen (oxygen free) starting 24 h before and during the measurement in order to minimise the effect of carbon dioxide and water vapour absorbance in its optical path. The latter is of critical importance for the IR analysis of a weak chromophore such as LGA. The background spectrum for the ATR probe was recorded in air at room temperature. The reasons for this are explained in ref 18.

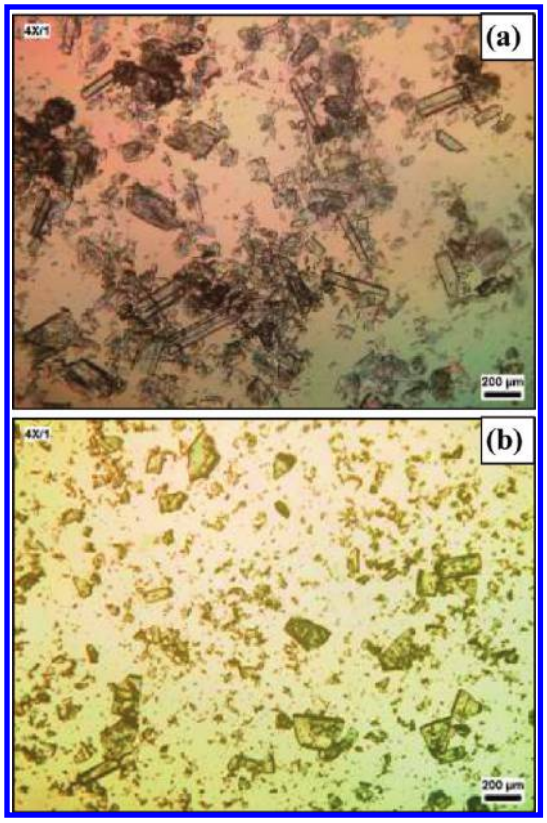

Figure 4. Microscopic images of (a) crushed seeds ($D_{0.5}$ = 78 μm and $D_{4,3}$ = 119 μm) and (b) dry milled seeds ($D_{0.5}$ = 40 μm and $D_{4,3}$ = 48 μm) of β-LGA used in pilot-plant experiments.

The batch cooling crystallisation experiments at both 20- and 250-L scale were carried out by seeding the solution within the metastable zone to provide the nuclei for the subsequent growth process.[18] Two types of seeds were used, namely the dry seeds and slurry seeds. The seed crystals were taken from the same batch of β-LGA used for the preparation of solutions, and the amount of seeds was 5% of the feed crystals used for the preparation of solution. For the experiments in the 20-L crystalliser, the size of seed crystals was the same as supplied by VWR International ($D_{0.5}$ = 132 μm and $D_{4,3}$ = 196 μm, see Figure 1b), whereas for the 250-L crystalliser crushed ($D_{0.5}$ = 78 μm and $D_{4,3}$ = 119 μm) and dry milled ($D_{0.5}$ = 40 μm and $D_{4,3}$ = 48 μm) crystals were used, as shown in Figure 4. The different seeding policy reflected the need to increase the surface area for the larger-scale size whilst maintaining the same mass fraction. Two methods of seeding, as described below, were used: internal seeding and external seeding, with the former being used for the preliminary work to optimise processing conditions.

In all crystallisation experiments, the initial LGA aqueous solution concentration was 62.5 g/L with corresponding saturation temperature with respect to β-LGA solubility of 78.9 °C.

The LGA-water slurry was prepared at room temperature and heated to 90 °C, with the temperature maintained constant for ca. 60 min to ensure dissolution of all the crystals. Prior to seeding, the solution temperature was reduced at a rate of 0.3 °C/min and the seed crystals, dry or in slurry, were added to the solution when the temperature reached a predetermined level within the metastable zone, ~77.6 °C. The solution was held at this temperature for ~60 min to reach equilibrium between the seed material and the solution at which the supersaturation is taken as unity. This method of seeding is referred to as the external seeding. The solution was cooled further at the same rate in order to bring the supersaturation level within the prescribed upper and lower limits of the supersaturation set-point. Once the supersaturation was set roughly between these limits, the control system was activated. The crystallisation process continued at cooling rates determined by the control algorithm until the solution temperature reached a prescribed limit, usually 25 °C. Some initial experiments were carried out using the alternative internal seeding method. In this method, the slurry was heated from room temperature to a predetermined temperature, which was below the saturation point corresponding to the initial solution concentration, needed to dissolve ~95% LGA crystals and thus leave ~5% crystals as seeds within the saturated solution. The saturated slurry was held at this temperature for about 2 h to reach equilibrium.

3. SUPERSATURATION CONTROL METHODOLOGY

3.1. Closed-Loop Control Strategy. The supersaturation control strategy and the associated algorithm were developed from that described by Grön et al.[3] Schematic diagrams of the supersaturation control system and its underpinning calculation algorithm are presented, respectively, in Figures 5 and 6 and which has the following variable parameters:

- supersaturation set-point (S_{set}),
- maximum allowed supersaturation (S_{max}),
- minimum allowed supersaturation (S_{min}),
- base-cooling rate $(dT/dt)_{Base}$ of the solution,
- incremental decrease $[\Delta(dT/dt)_D]$ to solution cooling rate if $S > S_{max}$,
- incremental increase $[\Delta(dT/dt)_I]$ to solution cooling rate if $S < S_{min}$,
- controller response time (Δt),
- polynomial fitting constants for the definition of solubility.

In this feedback strategy, the solution supersaturation (expressed as $S = C/C^*$) is controlled at a constant level by controlling the solution temperature profile via manipulating the crystalliser cooling and heating rates. The control algorithm uses two limiting values of the supersaturation, S_{min} and S_{max}, and tries to maintain the supersaturation within these limits. The values of S_{min} and S_{max} are usually chosen to be close to each other so that the supersaturation level remains practically constant during the crystallisation process. The supersaturation is maintained within these limits using the control algorithm as follows: if $S < S_{min}$, the solution temperature is reduced which causes a decrease in C^* and correspondingly, an increase in S; if $S > S_{max}$, then the temperature is raised which causes an increase in C^* and correspondingly, a decrease in S. At each time increment (Δt), the measured supersaturation is checked against the S_{min} and S_{max} values and if $S < S_{min}$, then the base-cooling rate is increased by $(dT/dt)_{Base} + \Delta(dT/dt)_I$, and if $S > S_{max}$, then the cooling rate is reduced by $(dT/dt)_{Base} - \Delta(dT/dt)_D$. If the supersaturation is between the upper and lower limits, there is no need to change the cooling rate.

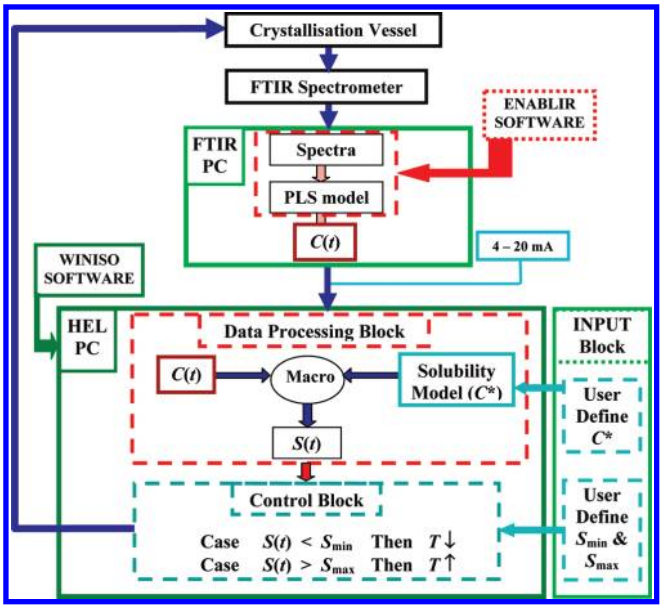

Figure 5. Schematic diagram of the supersaturation control system implemented in the HEL reactor control software for the 20-L crystalliser.

The above-mentioned parameters required for the control algorithm are defined as follows. The constants of the polynomial for solubility are obtained from a fourth-order polynomial based on the measured solubility:[18] $C^* = 4.408 - 0.146T + 0.018T^2 - 2.964 \times 10^{-4}T^3 + 2.682 \times 10^{-6}T$.[4] The supersaturation limits, S_{min} and S_{max}, are defined based on the self-prediction error of the PLS calibration model, which is in the range 1−10%.[18] A suitable initial base-cooling rate was applied to the solution at the start of the control step, which was chosen by examining the supersaturation profiles obtained in linear cooling runs at different rates. The response time (Δt) represents the time interval for the control action and is defined on the basis of the acquisition time of spectral data by the ATR-FTIR spectrometer for the prediction of online solution concentration. The supersaturation set-point was set to a desired value (S = 1.1, 1.2, 1.3, or 1.4).

3.2. Implementation of Control System. *3.2.1. In 20-L Crystalliser.* A cascade control system was used containing two control loops: crystalliser solution temperature (T_r) control and crystalliser jacket oil temperature (T_j) control. The supersaturation control was achieved through effecting solution temperature changes according to the strategy described above. The control algorithm was implemented by modifying the program *macro* in the HEL WinISO reactor control software used for the 20-L AUTOLAB crystalliser, as shown in Figure 5. The *macro* calculates the new supersaturation value using the LGA concentration data obtained from the ATR-FTIR spectrometer and the equilibrium concentration from the solubility model. The PLS calibration model was implemented in the control system via the EnablIR software. In the HEL reactor control scheme, the new set-point for the crystalliser solution temperature ($T_{r,set}$) is calculated by the control algorithm (see Figure 6) using the defined values of the above-mentioned control parameters. The original WinISO PI controller was used for the calculation of the required cooling rate and its transformation to a jacket oil temperature for the Huber heater/chiller unit.

dx.doi.org/10.1021/op100223a |*Org. Process Res. Dev.* 2011, 15, 540–555

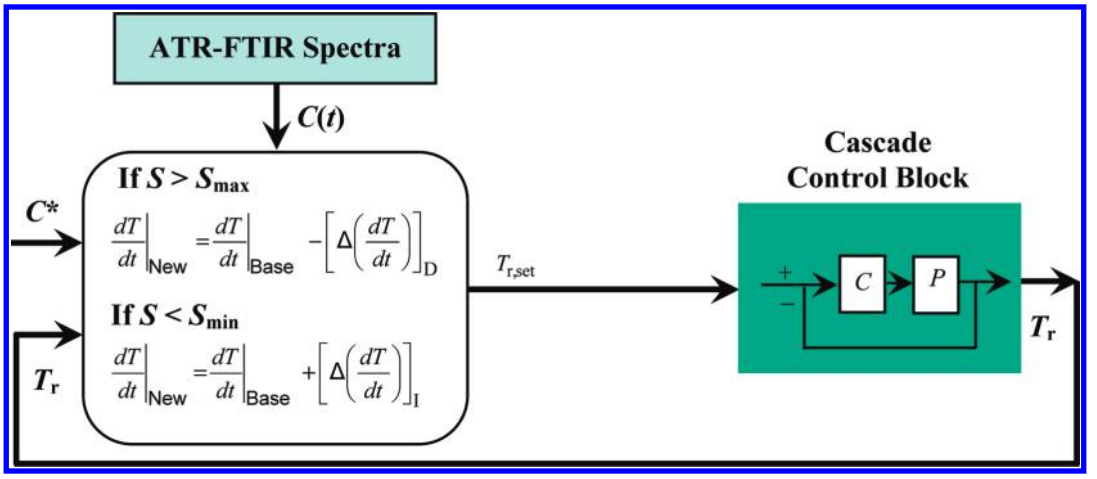

Figure 6. Schematic diagram of the supersaturation control algorithm used in the 20- and 250-L crystallisers.

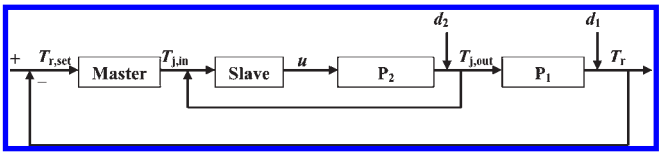

Figure 7. Conventional cascade control structure for the pilot-plant at Syngenta, Switzerland.

3.2.2. In 250-L Pilot-Plant Crystalliser. The pilot-plant at Syngenta, Münchwillen, has a conventional cascade control structure (Foxboro system) as shown in Figure 7. However, mindful of GMP and process safety considerations, this control system was not directly utilised for the supersaturation control trials. Instead, the control system, as described above and shown in Figure 6, was implemented as a MATLAB-based control program running on a standalone PC communicating with the Foxboro system through an MS Excel spreadsheet interrogated by both the Foxboro and the control PC system.

The 250-L system controllers were designed on the basis of the Internal Model Control (IMC) tuning techniques for ramp types of inputs. The control-loop block diagram of the pilot-plant crystalliser control system developed is shown in Figure 7 in which Process 1 (P_1) represents the dynamic behaviour between the crystalliser solution temperature (T_r) and the jacket outlet temperature ($T_{j,out}$), and Process 2 (P_2) is the dynamic behaviour between $T_{j,out}$ and the jacket inlet temperate ($T_{j,in}$). In this, P_i is the lumped dynamic model between u and $T_{j,out}$, where u is the manipulated variable, which is the valve position. The slave controller was designed as a proportional (P) controller, whereas the master controller was PI. Experimental data[19] from initial trials on the heating/cooling of water were used for developing a control model for the system as a MATLAB-based control program running on a standalone PC. The advantage of this hybrid approach is that the pilot-plant safety-validated control system is not compromised by the action of the external control PC, thus enabling safe running; e.g. if there were to be a control PC software/hardware failure, then the plant would still be under control within predefined safe operability.

The required measurements for the control strategy such as LGA concentration, T_r, $T_{j,in}$ and $T_{j,out}$, were all collected, and the control output was calculated in the supersaturation control PC using MATLAB. Figure 8 shows the communication between the control PC and the Foxboro Server via the Connoisseur OPC client connection. This is in the form of a MS Excel *macro*, which is linked to the OPC client through a dynamic library. The structure of the connection is shown in Figure 9. By using this approach, inadvertent shutting down of the MATLAB control code, during experimental runs, does not cause any break in the communication between the two computers.

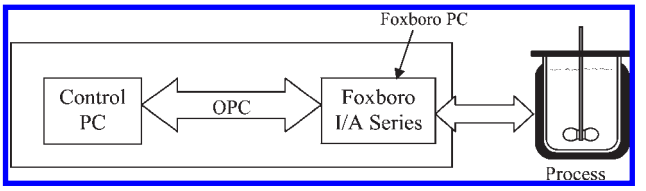

Figure 8. Communication scheme between the supersaturation control PC and the Foxboro computer in the pilot-plant.

4. RESULTS AND DISCUSSION

A series of controlled seeded crystallisation experiments was carried out using the control system together with ATR-FTIR spectrometer initially in the 20-L laboratory-scale crystalliser, which also included optimisation of the control algorithm parameters, and then in the industrial pilot-plant. Uncontrolled crystallisation experiments were also carried out in the 20-L scale-size as a reference point. The experimental conditions are given in Table 1. The average cooling rate (dT/dt) and the overall rate of solute consumption (dC/dt) were calculated from the measured solution temperature and concentration profiles, respectively, over the period of controlled supersaturation for each run and given in Table 1. Data of representative experiments (three runs in the 20-L and four runs in the 250-L crystalliser) are presented below, detailed results of all the experiments conducted may be found in ref 20.

4.1. Uncontrolled Supersaturation Crystallisation at 20 L. A crystallisation experiment (run 1) without supersaturation control using the dry external seeds at a constant cooling rate of 0.3 °C/min was carried out following the same protocol as that used for controlled crystallisation experiments. Figure 10a shows the variation of measured LGA concentration, supersaturation, and the solution and jacket oil temperature profiles as a function of time. In order to avoid cluttering of the graph, the measured

dx.doi.org/10.1021/op100223a |*Org. Process Res. Dev.* 2011, 15, 540–555

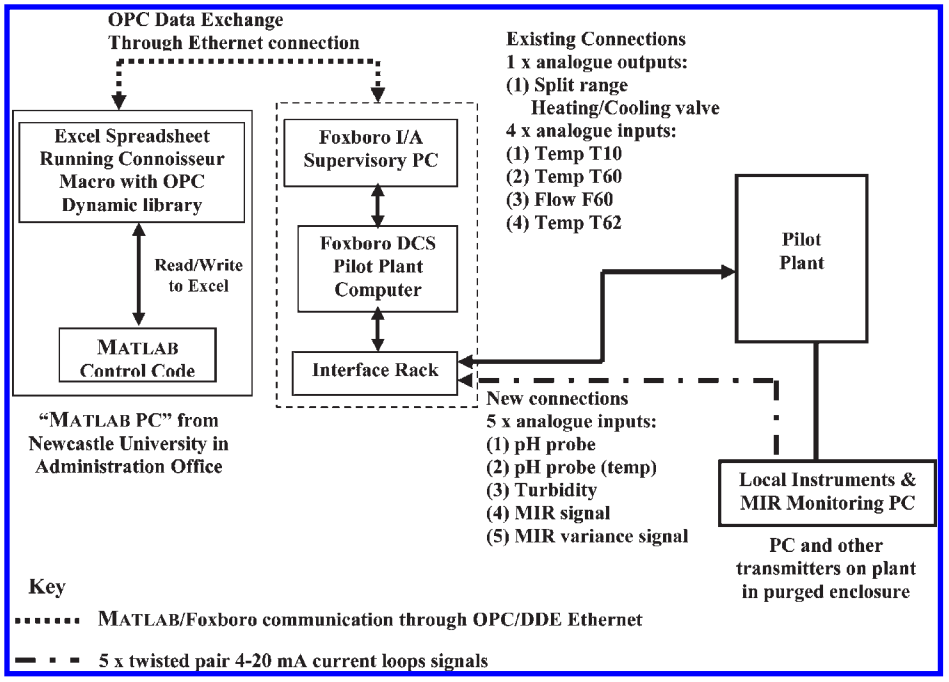

Figure 9. Schematic layout of control communications used for controlling the pilot-plant crystalliser.

Table 1. Experimental conditions for seeded batch cooling crystallisation of LGA with/without supersaturation control in 20- and 250-L crystallisers

			supersaturation				seed size [μm]		product crystal size [μm]		av cooling rate (dT/dt)	rate of depletion of solute conc.	duration of
run	crystalliser size [L]	mode of seeding[a]	S_{min}	S_{set}	S_{max}	S_{avg}	$D_{0.5}$	$D_{4,3}$	$D_{0.5}$	$D_{4,3}$	[°C/min]	(dC/dt) [g/L·min]	S-control [h:min]
1	20	external (dry)	uncontrolled S_{max} = 1.33				132	196	N/A	N/A	0.3	0.34	–
2	20	external (dry)	1.075	1.1	1.125	1.09	132	196	204	N/A	0.105	0.133	5:00
3	20	internal	1.175	1.2	1.225	1.16	N/A	N/A	146	N/A	0.119	0.215	2:00
4	250	external (slurry)	1.075	1.1	1.125	1.1	78	119	115	248	0.020	0.032	15:00
5	250	external (slurry)	1.175	1.2	1.225	1.2	78	119	94	214	0.083	0.101	13:00
6	250	external (slurry)	1.275	1.3	1.325	1.28	78	119	88	206	0.174	0.211	7:30
7	250	external (slurry)	1.175	1.2	1.225	1.2	40	48	74	120	0.076	0.109	3:50

[a] 5% seeds were added at 77.6 °C in all runs. N/A = Data not available.

turbidity and pH profiles are omitted from the figure. The PLS model accurately predicts the initial concentration of the solution prior to seeding. As can be seen, following the addition of seed crystals at about 160 min, the solution concentration initially decreases rather rapidly and then becomes almost constant during the 60-min interval when the solution temperature is held constant. At the end of this period, a cooling rate of 0.3 °C/min is applied at around 225 min, and the solution is cooled at this rate during the rest of the crystallisation process. It can be seen that the LGA concentration starts to decrease and eventually reaches a value of 16.0 g/L at the end of the process. The corresponding supersaturation profile shows an initial rapid increase up to a peak level of 1.3, suggesting that the applied cooling rate is sufficiently high to generate supersaturation, which exceeds the desupersaturation rate resulting from the consumption of solute due to the growth of seed crystals. This is followed by an initial slow and later somewhat rapid desupersaturation due to the consumption of solute resulting from secondary nucleation and the growth of the freshly generated solids as well as the seed crystals. The occurrence of secondary nucleation is evident from the presence of fine particles in the final product crystals, as shown in the optical microscopic image in Figure 10b. This image also confirms the formation of needle-like β-LGA crystals. It should be noted that there was no strong evidence of breakage from the optical microscopic images of needle-like crystals produced in the laboratory-sale and pilot-plant crystallisers for the agitation rate used.

4.2. Controlled Supersaturation Crystallisation at 20 L. A number of controlled crystallisation experiments were carried out in the 20-L crystalliser initially to test the implementation of the supersaturation control system and to optimise the parameters of the control algorithm in order to achieve a tight control of the supersaturation within the set limits, S_{min} and S_{max}, and to provide a basis for scaling up. Figure 11 shows the performance of the control system with initial values of the control parameters specified based on the guidelines given above. It can be seen that the supersaturation oscillates throughout the run significantly exceeding the S_{min} and S_{max} limits, and the solution temperature

dx.doi.org/10.1021/op100223a |*Org. Process Res. Dev.* 2011, 15, 540–555

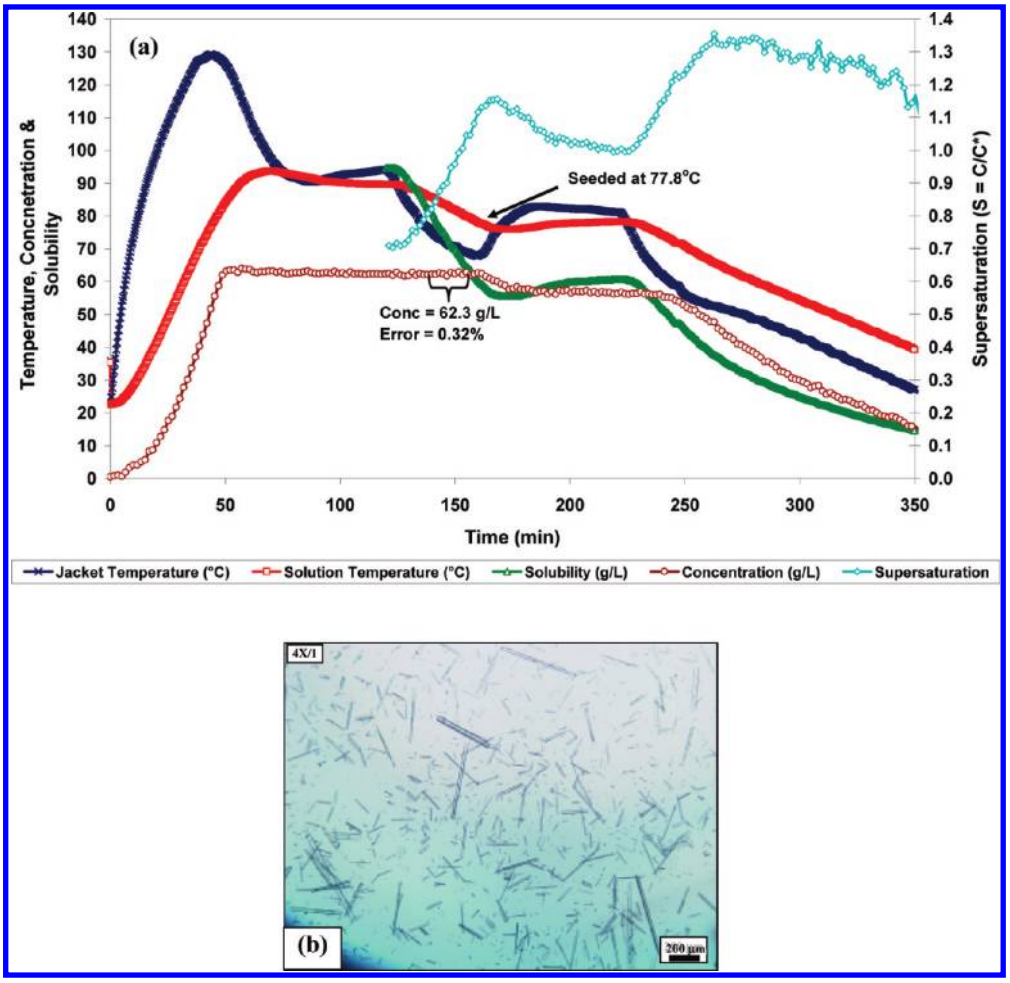

Figure 10. (a) Data of seeded crystallisation experiments (run 1) without supersaturation control at 0.3 °C/min cooling rate in 20-L laboratory crystalliser and (b) microscopic image of product crystals.

does not follow the crystalliser set-point temperature specified by the HEL reactor control software. Through further tuning of these parameters via a number of runs (for details see ref 20), it was possible to dampen the oscillations and to maintain the supersaturation level within the S_{min} and S_{max} limits. The optimised values of the control algorithm parameters are given in Table 2.

Data of a typical experiment (run 2) carried out with this set of parameters in which the supersaturation level was set to $S_{set} = 1.1$ using the external seeding method with dry seed crystals is shown in Figure 12. The performance of the control algorithm is revealed by the supersaturation profile as a function of time. It can be seen that the supersaturation is well controlled within the set limits, $S_{min} = 1.075$ and $S_{max} = 1.125$, with an average value of $S_{avg} = 1.09$ for about 5 h by continuously adjusting the crystalliser temperature, which follows a convex profile in agreement with the theoretically determined optimum cooling profiles reported in the literature.[5,6,14] As the crystallisation process proceeds, the surface area of the crystals increases due to the growth resulting in an increased rate of solute consumption. This necessitated higher cooling rates in order to maintain the constant level of supersaturation. However, towards the end of the process, the supersaturation starts to drop rather rapidly. In order to prevent this, the controller action resulted in a rapidly decreasing jacket oil temperature, as can be seen in Figure 12, but due to the dynamic limitations of the crystalliser cooling system the rate of cooling of the solution could not be maintained sufficiently high enough to enable the supersaturation to be kept within the prescribed range. Finally, the controller action stopped when the solution temperature reached its set limit of 25 °C.

Another crystallisation experiment (run 3), see Figure 13, was conducted with $S_{set} = 1.2$ using the internal seeding method, and the LGA-water slurry at 25 °C obtained from the previous batch (run 2). As shown in Figure 13, the supersaturation is controlled within $S_{min} = 1.175$ and $S_{max} = 1.225$ for ~2 h with an average $S_{avg} = 1.16$. The solution temperature decreases following a convex profile similar to that in run 2. Towards the end of this run, the process dynamics show similar trends as found in run 2. The experiment was stopped manually at a solution temperature ~54 °C as the supersaturation dropped much below the lower limit.

Optical microscopic images of the β-LGA crystals in slurries added as dry seeds and produced as internal seeds and the final product crystals for runs 2 and 3 are shown in Figure 14. In both the experiments, the growth of seeds is clearly evident from the presence of particles in the final product crystals which are larger than the seed particles, and also the average size of product crystals is larger compared with the seed size (see Table 1), although the size of internal seeds is not available. The existence of a large number of small crystals in the products, particularly in run 2, indicates the occurrence of secondary nucleation.

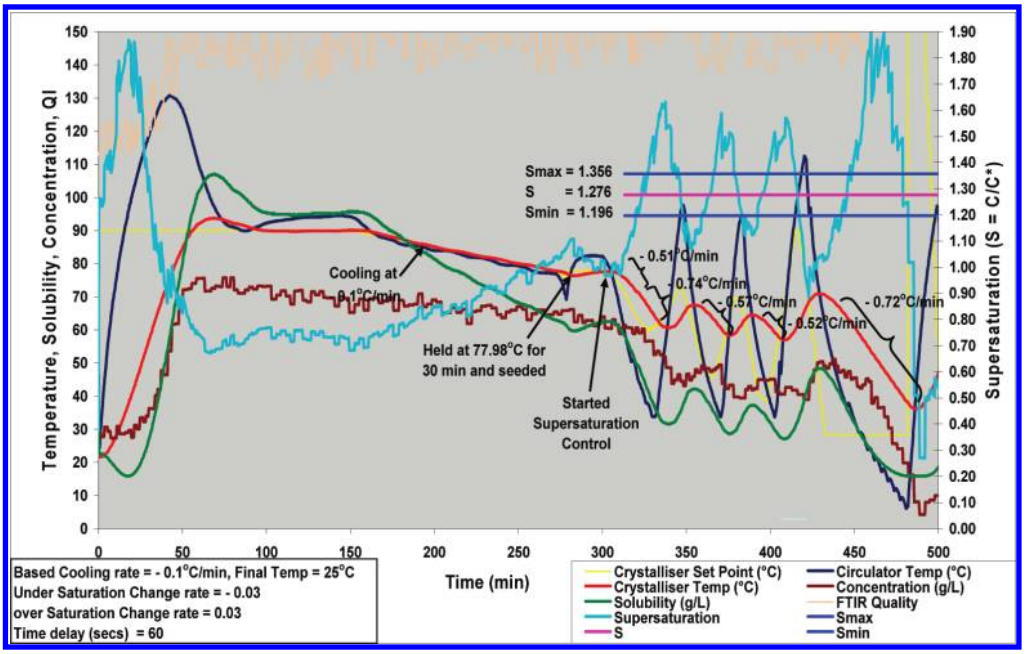

Figure 11. Data of an initial supersaturation control trial in the 20-L laboratory crystalliser using the following control algorithm parameters: base-cooling rate = −0.1 °C/min, under-/oversaturation change rates = ±0.03 (°C/min)/min, and response time = 60 s.

Table 2. Values of the supersaturation control algorithm parameters

crystalliser	ΔS^a (deviation from S_{set})	Δt [s]	$(dT/dt)_{Base}$[°C/min]	$\Delta(dT/dt)_I$[(°C/min)/min]	$\Delta(dT/dt)_D$[(°C/min)/min]
20-L	±0.025	110	0.10	0.001	0.001
pilot-plant	±0.025	110	0.12	0.01	0.01

[a] $S_{min} = S_{set} - \Delta S$ and $S_{max} = S_{set} + \Delta S$.

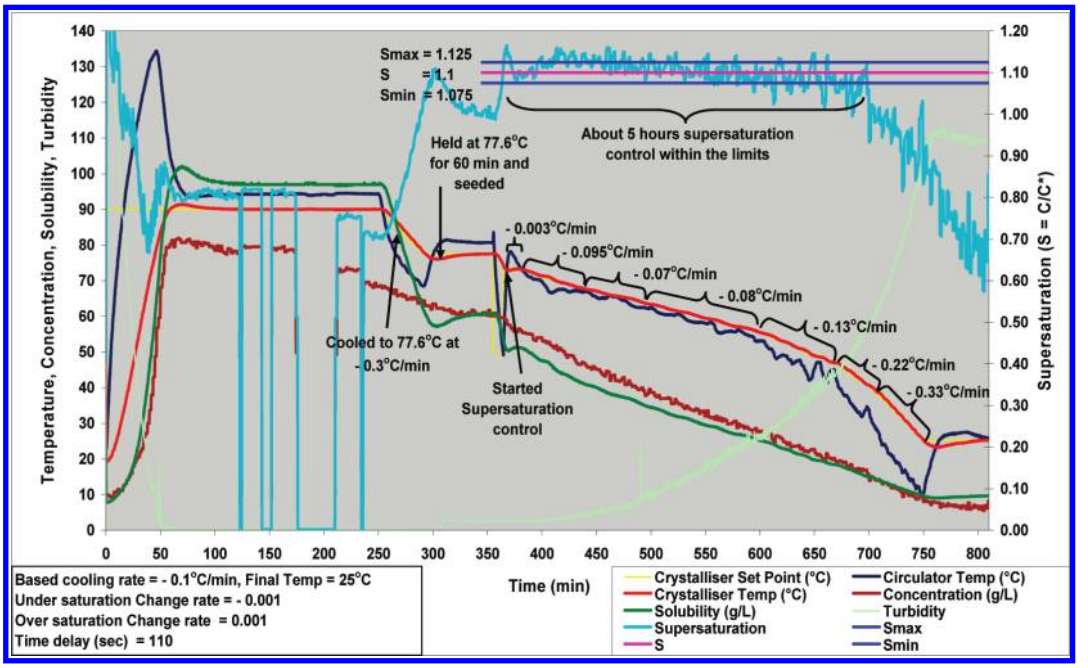

Figure 12. Data of supersaturation control experiment (run 2) with external seeding at S = 1.1 in the 20-L laboratory crystalliser.

The average size of the product crystals obtained in run 2 with S_{avg} = 1.09 is 204 μm compared with 146 μm in run 3 with S_{avg} = 1.16; however, in the absence of data of the internal seeds produced in run 3 it is difficult to make a direct comparison between the product crystal sizes obtained from these runs only on the basis of the level of supersaturation. It is interesting to note

dx.doi.org/10.1021/op100223a |*Org. Process Res. Dev.* 2011, 15, 540–555

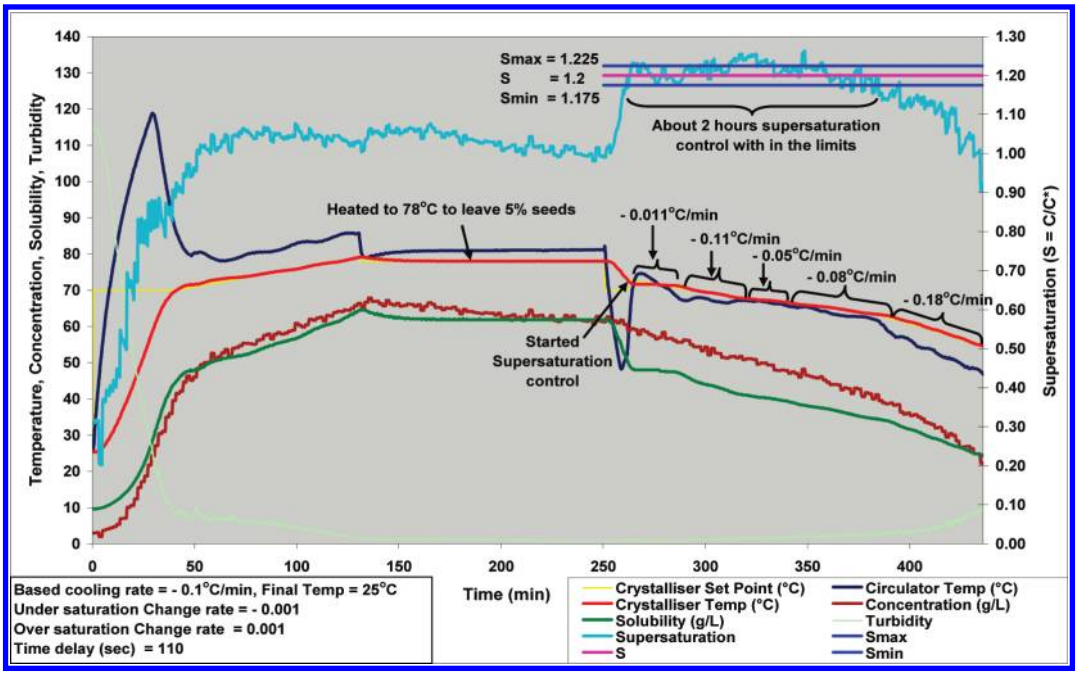

Figure 13. Data of supersaturation control experiment (run 3) with internal seeding at $S = 1.2$ in the 20-L laboratory crystalliser.

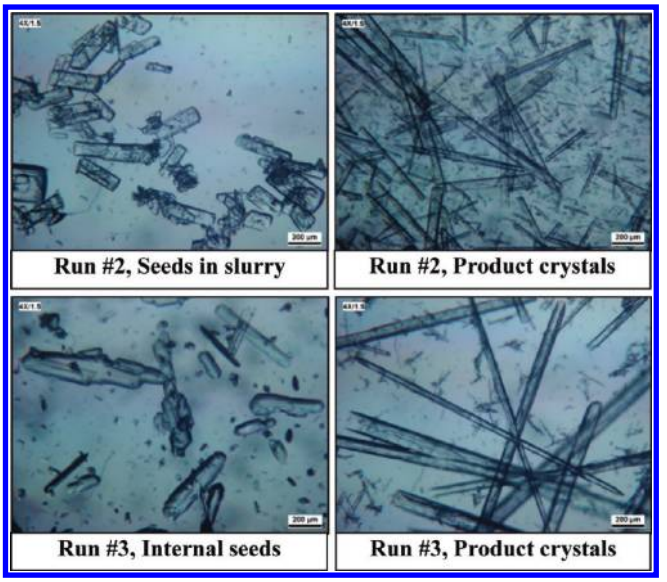

Figure 14. Microscopic images of β-LGA seeds in slurries and product crystals in the 20-L laboratory crystalliser for runs 2 and 3.

in Figure 14 that the fraction of small size crystals is higher in run 2, suggesting that secondary nucleation is more prevalent in the crystallisation with dry external seeding in spite of a lower level of supersaturation. This may be due to the CSD of external seeds being wider than that of the internal seeds because of finer particles generated by particle attrition. Also, enhanced secondary nucleation occurs for the external seeds due to high surface area compared with internal seeds. It is expected that internal seeds should have much smaller fraction of small particles because of potential dissolution on heating. Finally, a comparison of these images of the product crystals with those produced in crystallisation without supersaturation control (run 1, Figure 10) reveals that in run 1 very fine needle-like crystals are produced with a smaller average size.

4.3. Controlled Supersaturation Crystallisation at 250 L.

The control algorithm parameters optimised at the 20-L scale-size (see Table 2) provided a basis for the supersaturation control experiments carried out in the 250-L crystalliser in order to demonstrate the scaling up performance of the control system. The data obtained in an initial run using the internal seeding method is shown in Figure 15. As can be seen, the supersaturation is maintained at a reasonably constant level, with the average supersaturation being 1.13, up to about 530 min, but below the set-point value which is S_{set} = 1.20. The analysis of the data suggested that the supersaturation can be maintained within the S_{min}/S_{max} limits by increasing the base cooling rate and by adjusting the incremental increase/decrease to cooling rate parameters to account for the scaling effect. Further experiments were carried out[20] to tune these parameters, which are given in Table 2. With the new set of values of control parameters, four trials were conducted with external seeding, which included three trials (runs 4−6) using crushed β-LGA seeds ($D_{0.5}$ = 78 μm) in slurry and one (run 7) with dry milled seeds ($D_{0.5}$ = 40 μm) in slurry, as shown in Figure 4. Details of these runs are given in Table 1.

Figures 16−18 show the data obtained from runs 4−6 in which the supersaturation was maintained constant at 1.1 (±0.025), 1.2 (±0.025), and 1.3 (±0.025), respectively. In all these runs, as the seed slurry was added to the solution, the LGA concentration started to decrease due to the consumption of solute molecules by the growth of the seed crystals and also via secondary nucleation and the growth of freshly generated solids, depending on the supersaturation level. The performance of the control algorithm is revealed by the supersaturation profile as a function of time, which shows that the supersaturation in these runs is generally well maintained within the prescribed S_{min} and S_{max} range, with average values very close to the supersaturation set-points (see Table 1). However, as the supersaturation level increases, so does the fluctuation around the set-points, suggesting that the control algorithm parameters may require further adjustment. The LGA concentration profiles in Figures 16−18 show that initially the rates of consumption of solute are high which require high cooling rates in order to maintain the desired

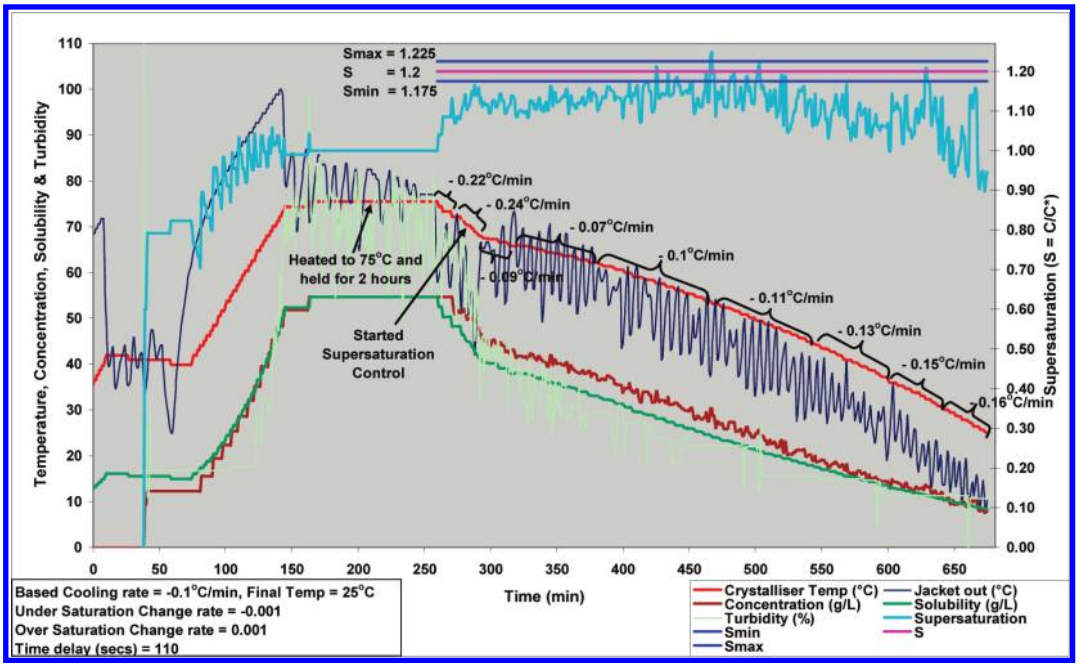

Figure 15. Data of an initial supersaturation control trial in the 250-L pilot-plant crystalliser using the internal seeding method with the following control algorithm parameters: base cooling rate = −0.1 °C/min, under-/oversaturation change rates = ±0.001 (°C/min)/min, and response time = 110 s.

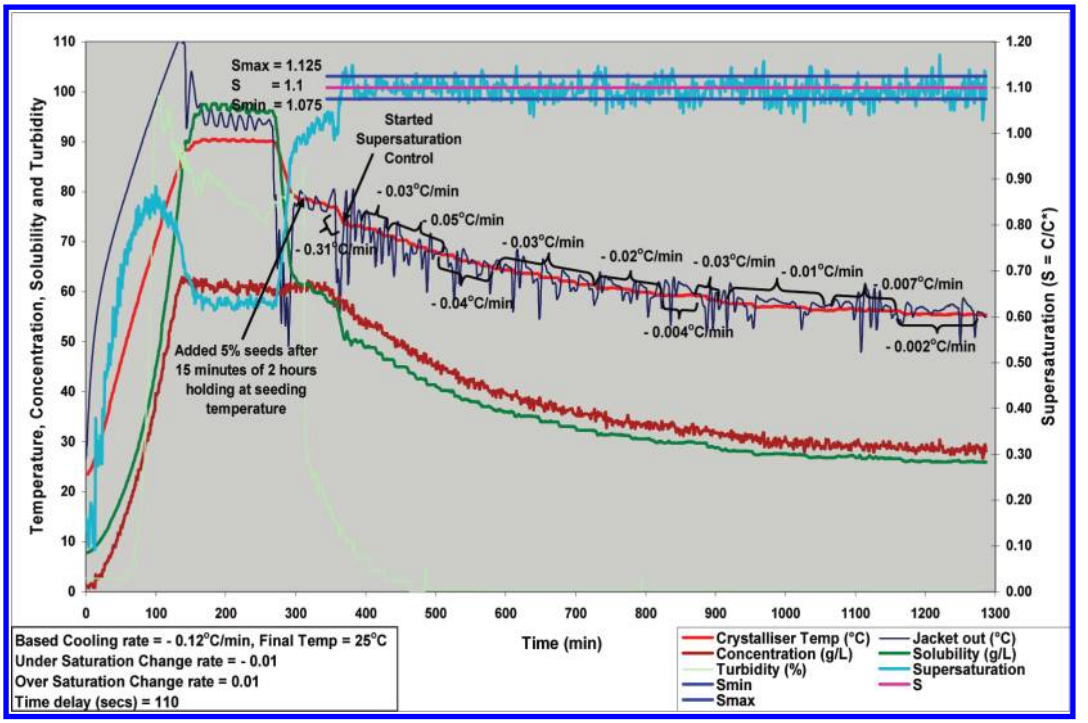

Figure 16. Data of supersaturation control experiment (run 4) with external seeding (crushed seeds) at $S = 1.1$ in the 250-L pilot-plant crystalliser.

levels of supersaturation, but the solute consumption rate gradually reduces, and hence the cooling rate, as the crystallisation progresses. This trend is contrary to that found at the 20-L scale-size, as shown in Figures 12 and 13. The reason for this is not clear and hard to discern from the current experimental data, mindful that the mean size and CSD of seeds differ due to operational conditions not being the same. In the 250-L vessel, it can be seen from Table 1 that the overall rate of depletion of solute and the average cooling rate increase with increasing supersaturation level, as expected. However, the rates of depletion of solute in the 20-L vessel (runs 2 and 3) are higher compared with those in the 250-L scale (runs 4 and 5), in spite of the available surface area of the seed crystals being less due to larger seed size; consequently, higher cooling rates are needed in the smaller-size vessel in order to maintain the same levels of supersaturation. This is consistent with the occurrence of secondary nucleation presumably via the contact mechanism at the 20-L scale-size in which the total

dx.doi.org/10.1021/op100223a |*Org. Process Res. Dev.* 2011, 15, 540–555

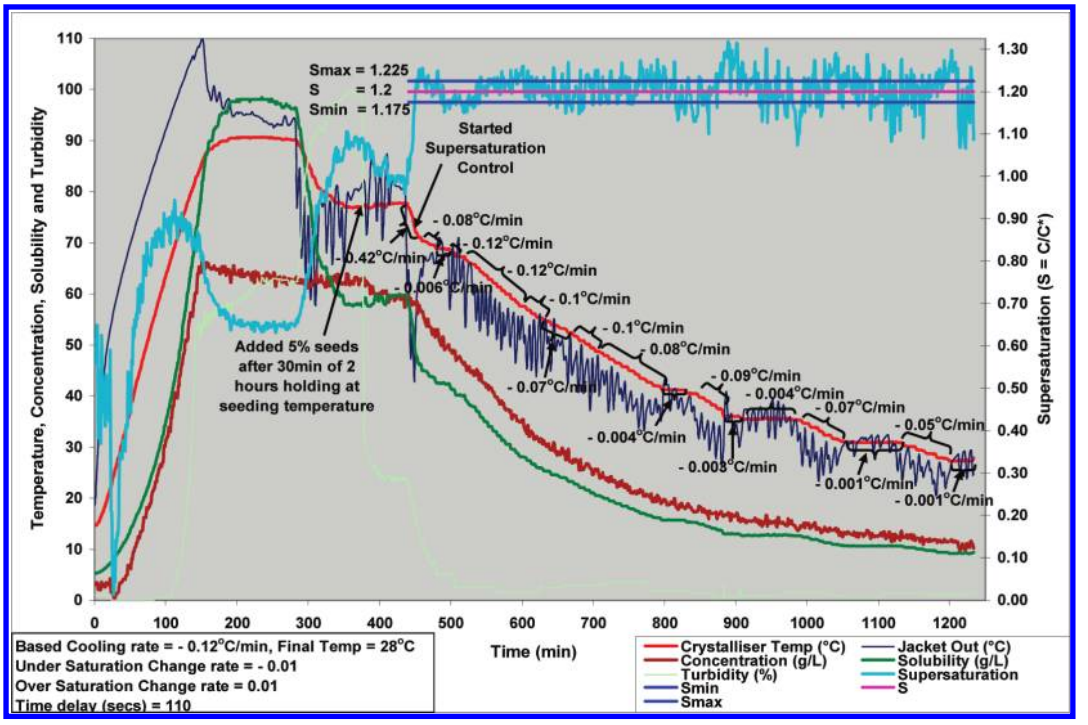

Figure 17. Data of supersaturation control experiment (run 5) with external seeding (crushed seeds) at S = 1.2 in the 250-L pilot-plant crystalliser.

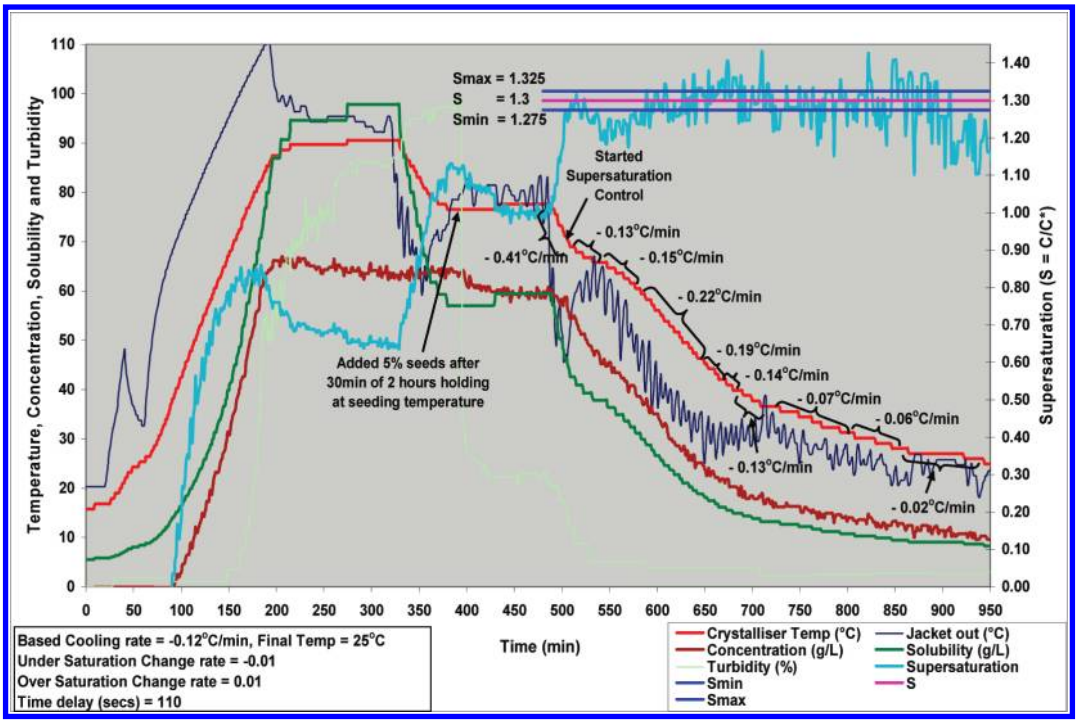

Figure 18. Data of supersaturation control experiment (run 6) with external seeding (crushed seeds) at S = 1.3 in the 250-L pilot-plant crystalliser.

surface area (including the surfaces of the vessel and probes) per unit volume of the crystalliser is much larger, 0.019 m^2/L, compared with 0.009 m^2/L in the 250-L crystalliser. This hypothesis is supported by the microscopic images of product crystals obtained in the two scale sizes, as shown in Figure 20, which is discussed further below.

In run 7 (see Figure 19), the seed size was reduced to 40 μm, but the amount remained constant, and the supersaturation set-point was fixed at 1.2 to examine the effect of the size of seeds, that is, the particle surface area available initially, on the crystallisation process. In this run the supersaturation was controlled for more than 3 h. The experiment was stopped early due to plant shut down when the solution temperature reached ~57 °C. A comparison of the data from this run with that from run 5 (S_{set} = 1.2), given in Table 1, shows that the average solute consumption rate is slightly higher and the solute concentration is slightly lower following the addition of seeds (not shown here) in run 7.

dx.doi.org/10.1021/op100223a |*Org. Process Res. Dev.* 2011, 15, 540–555

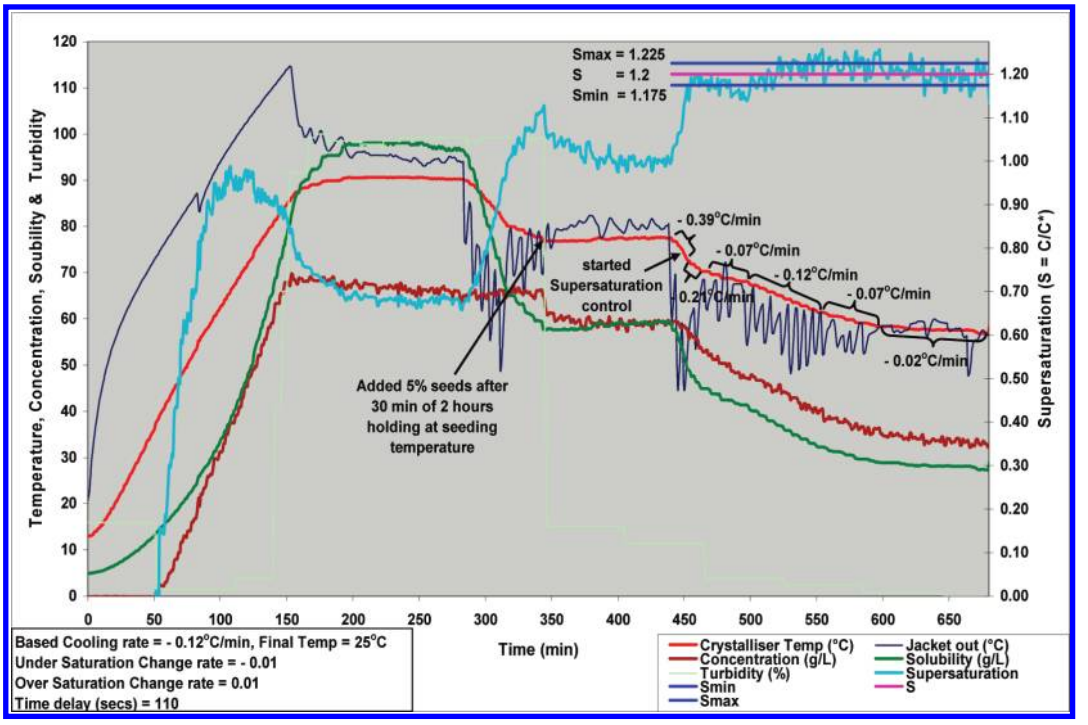

Figure 19. Data of supersaturation control experiment (run 7) with external seeding (milled seeds) at $S = 1.2$ in the 250-L pilot-plant crystalliser.

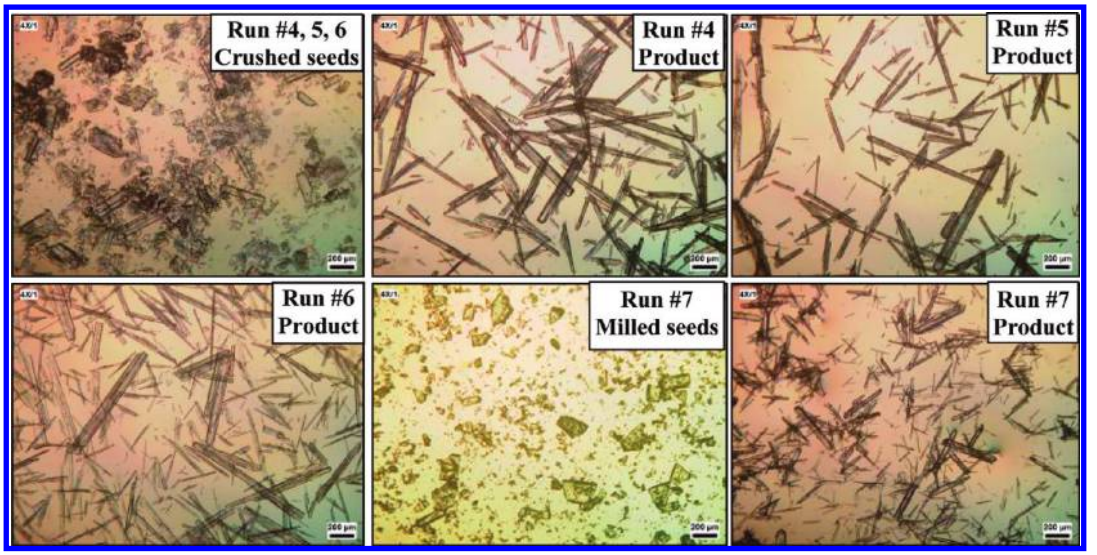

Figure 20. Microscopic images of β-LGA seeds in slurry and product crystals in the 250-L pilot-plant crystalliser.

Microscopic images of the seeds in slurry and the final product crystals for runs 4−7 in the pilot-plant crystalliser are shown in Figure 20. It can be seen that needle-like β-LGA crystals are produced in all runs. For the same size of seeds (runs 4−6), the product crystal size decreases with increasing supersaturation level. The growth of seeds in these runs is evident as revealed by the larger product crystal sizes compared with the seed size given in Table 1. The presence of fine particles in the products obtained for the highest supersaturation (run 6), $S_{set} = 1.3$, reveals that fresh nuclei are produced via secondary nucleation. The images of runs 5 and 7 show the effect of seed size, that is, the resulting initial surface area of the seeds, on the final product crystals at the same supersaturation level. Crystals obtained in run 7 with a smaller seed size show a much larger fraction of fine particles compared with run 5 in which larger seeds were used. This is indicative of the occurrence of secondary surface nucleation due to the availability of more surface area.[21] However, the possibility that the surfaces of the milled seeds might have been damaged during milling, which inhibited growth, cannot be ruled out conclusively. A comparison between the crystals produced using the external seeding method at the 20-L scale-size (run 2) with those at the 250-L scale for the same (run 4) or even higher (runs 5 and 6) supersaturation levels indicates that secondary nucleation is more prevalent at the smaller-scale size. This is consistent with that observed in seeded batch cooling crystallisation without supersaturation control carried out at 500-mL and 20-L scale sizes in our previous study.[18]

dx.doi.org/10.1021/op100223a |*Org. Process Res. Dev.* 2011, 15, 540–555

5. CONCLUSIONS

The closed-loop supersaturation control system[3] with ATR-FTIR using a univariate peak-ratio calibration model applied to the spontaneous crystallisation of MSG at the 500-mL scale-size has been further developed by extending the studies to a seeded process and coupling this approach with a multivariate chemometric PLS calibration model to enable studies of the weak chromophore LGA which was then scaled up to 20- and 250-L sizes. Supersaturation control experiments were carried out on seeded batch cooling crystallisation of LGA from aqueous solutions using both internal and external seeding modes. The supersaturation control system was initially applied to maintain the supersaturation at different levels within a prescribed range in the laboratory-scale 20-L crystalliser at Leeds and the control algorithm parameters were optimised. The supersaturation monitoring/control system was then implemented in a 250-L industrial pilot-plant crystalliser at Syngenta, Münchwillen, Switzerland, and series of trials were performed at three supersaturation levels: 1.1, 1.2, and 1.3 using both crushed and milled seeds. Good control of supersaturation within the set upper/lower limits was achieved by continuously adjusting the solution temperature and cooling rate.

In both laboratory and pilot-plant experiments needle-like stable β-LGA crystals were produced. The average size of final product crystals decreases with increasing supersaturation. Analysis of the CSD for the product crystals is consistent with the occurrence of secondary nucleation, the extent of which depends on the supersaturation level, in addition to the growth of seeds, with the latter being more prevalent at the smaller-scale size. This is consistent with our previous observation in seeded crystallisation of LGA without supersaturation control in 500-mL and 20-L crystallisers.[18] For the same level of supersaturation, the rate of depletion of solute was faster at the 20-L scale-size than at the 250-L scale, and hence, a higher cooling rate was required to maintain the desired supersaturation. However, at a given scale size, as expected, the average cooling rate required to maintain a constant supersaturation increased with increasing supersaturation level.

The present study has demonstrated that it is possible to control supersaturation at different levels associated with the crystallisation of a challenging compound in an industrial-scale crystalliser overcoming a range of practical challenges based on optimised values of the control parameters at a laboratory scale. The crystallisation control strategy and system described here has been further developed using a more advanced chemometric methodology[22] and through the further development of control strategy incorporating an improved PI approach, with the latter successfully demonstrated at both the 20- and 250-L scale.[20] The latter will form the basis for a further publication. The overall supersaturation control methodology is currently being applied for controlling the crystallisation process of a commercial compound of Syngenta from impure mother liquor replicating the industrial production process.

The current supersaturation control system can, in principle, be extended to antisolvent and evaporative crystallisation processes with appropriate modifications. For the former process, the feedback control algorithm needs to be modified for controlling the antisolvent addition rate instead of the solution temperature profile, whilst for the latter process this requires feedback control including heat transfer to the crystalliser with respect to the mass of the solvent evaporated.

AUTHOR INFORMATION

Corresponding Author

*Telephone: +44 (0) 113 233 2431. Fax: +44 (0) 113 233 2405. E-mail: T.Mahmud@leeds.ac.uk

Present Addresses

[†]Pfizer Global Research & Development, Ramsgate Road, Sandwich, Kent CT13 9NJ, U.K.

[‡]IPCOS, Bosscheweg 135b, 5282 WV Boxtel, The Netherlands.

[§]Syngenta Sensors University Innovation Centre, School of Electrical and Electronic Engineering, University of Manchester, Manchester M13 9PL, U.K.

ACKNOWLEDGMENT

This work has been carried out as part of *Chemicals Behaving Badly* Phase 2, a collaborative project funded by the U.K. Science and Engineering Research Council (EPSRC) together with support from an industrial consortium including ANSYS Europe Ltd, AstraZeneca, Bede Scientific Instruments Ltd., BNFL, Clairet Scientific Ltd., GlaxoSmithKline, HEL Ltd., Malvern Instruments, Pfizer, and Syngenta. The academic partners are Leeds, Heriot-Watt, and Newcastle Universities. We gratefully acknowledge all these sponsors and all members of this academic/industrial team, notably industrial coordinator Leslie J. Ford, Xiaojun Lai (Leeds), Ivan Marziano (Pfizer), and Alan Donnelly (Heriot-Watt University) for helpful discussions and Steve Caddick (Leeds) for technical support.

NOMENCLATURE

C = solute concentration [g/L]
C^* = equilibrium concentration [g/L]
$D_{0.5}$ = mean particle diameter [μm]
$D_{4,3}$ = volume weighted mean particle diameter [μm]
Re = Reynolds number [-]
S = supersaturation [-]
S_{set} = supersaturation set-point [-]
S_{max} = maximum allowed supersaturation [-]
S_{min} = minimum allowed supersaturation [-]
T = temperature [°C]
T_j = crystalliser jacket oil temperature [°C]
T_r = solution temperature [°C]
Δt = controller response time [s]

ABBREVIATIONS

ATR-FTIR Attenuated total reflection - Fourier transform infrared
CSD Crystal size distribution
LGA L-glutamic acid
MSG Monosodium glutamate
PI Proportional-integral
PLS Partial least-squares

REFERENCES

(1) Mersmann, A. *Chem. Eng. Process* **1999**, *38*, 345–353.
(2) Braatz, D. R. *Annu. Rev. Control* **2002**, *26*, 87–99.
(3) Grön, H.; Borrisova, A.; Roberts, K. J. *Ind. Eng. Chem. Res.* **2003**, *42*, 198–206.
(4) Tavare, N. S. *Industrial Crystallization Process: Simulation Analysis and Design*; Plenum Press: New York, 1995.
(5) Mullin, J. W.; Nyvlt., J. *Chem. Eng. Sci.* **1971**, *26*, 369.
(6) Jones, A. G.; Mullin, J. M. *Chem. Eng. Sci.* **1974**, *29*, 105.

(7) Jagadeshi, D.; Kubota, N.; Yokota, M.; Sato, A.; Tavare, N. S. *J. Chem. Eng. Jpn.* **1996**, *29*, 865–873.
(8) Ulrich, J.; Strege, C. *J. Cryst. Growth* **2002**, *237*−*239*, 2130–2135.
(9) Pollanen, K.; Hakkinen, A.; Reinikainen, S.-P.; Louhi-Kultanen, M.; Nystrom, L. *Chem. Eng. Res. Design* **2006**, *84*, 47–59.
(10) Myerson, A. S.; Decker, S. E.; Welplng, F. *Ind. Eng. Chem. Process Des. Dev.* **1986**, *25*, 925–929.
(11) Moscosa-Santillan, M.; Bals, O.; Fauduet, H. C.; Porte, A. *Chem. Eng. Sci.* **2000**, *55*, 3759–3770.
(12) Srinivasakannan, C.; Vasanthakumar, R.; Iyappan, K.; Rao, P. G. *Chem. Biochem. Eng. Q.* **2002**, *16*, 125–129.
(13) Liotta, V.; Sabesan, V. *Org. Process Res. Dev.* **2004**, *8*, 488–494.
(14) Jones, A. G. *Chem. Eng. Sci.* **1974**, *29*, 1075.
(15) Davey, R.; Garside, J. *From Molecules to Crystallisers*; Oxford University Press Inc.: New York, 2000; pp 62−73.
(16) Feng, L; Berglund, K. A. *Cryst. Growth Des.* **2002**, *2*, 449–370.
(17) Fujiwara, M.; Chow, P. S.; Ma, D. L.; Braatz, R. D. *Cryst. Growth Des.* **2002**, *2*, 363–370.
(18) Borissova, A.; Khan, S.; Mahmud, T.; Roberts, K. J.; Andrews, J.; Dallin, P.; Chen, Z. P.; Martin, E.; Morris, J. *Cryst. Growth Des.* **2009**, *9*, 692–706.
(19) Al-Ghafran, M.; Andrews, J.; Dallin, P.; Gibson, N.; Grieve, B.; Hall, A.; Khan, S.; Ma, C. Y.; Mahmud, T.; Morris, J.; Ozkan, L.; Penchev, R. Y.; Price, C. J.; Roberts, K. J. *Proceedings of the 7th World Congress of Chemical Engineering on CD-ROM*, IChemE, 2008.
(20) Khan, S. *Application of On-line ATR-FTIR Spectroscopy for Monitoring, Controlling and Scaling-up the Batch Crystallisation of L-Glutamic Acid*, PhD Thesis, University of Leeds: UK, 2008.
(21) Oullion, M.; Puel, F.; Févotte, G.; Righini, S.; Carvin, P. *Chem. Eng. Sci.* **2007**, *62*, 820–832.
(22) Ping Chen, Z. P.; Morris, J.; Borissova, A.; Khan, S.; Mahmud, T.; Penchev, R.; Roberts, K. J. *Chemom. Intell. Lab. Syst.* **2009**, *96* (1), 49–58.